

# COMPILATION OF NEUTRON RESONANCE PARAMETERS NRF-3

Z.N.Soroko, S.I.Sukhoruchkin, D.S.Sukhoruchkin

Petersburg Nuclear Physics Institute, Gatchina, Russia

## 1 Introduction

The development of the atomic industry demands determination of parameters of nuclear reactions which take place in the reactor and in its fuel. The collection of neutron resonance parameters became a tradition after the Geneva Conference when International Atomic Energy Agency started supervision on nuclear data collection and distribution.

Resonance parameters were collected in BNL as the report BNL-325 (D.Hughes, J.Harvey, M.Goldberg, later S.Mughabghab) [1]. The long delay in 5-th BNL-325 Edition (planned for 2006 [1]) was partly compensated by compilations NRF-1,2 published by Landolt-Börnstein Library (LBL) Springer [2,3]. The Editor-in-Chief of LBL Group I.W.Martienssen noticed [4] that data compilations serve as bridges between different branches of science.

It concerns also NRF: resonance parameters from high-resolution cross section measurements needed for reactor calculations are used for a study of nuclear structure effects (fine and superfine effects, FS and SFS) seen in the energies of nuclear states. The file NRF-3 (updated NRF-2) is a part of a Combined Nuclear Reaction File (CNRF) [5] used for a study of "tuning effects" in nuclear data and particle masses [6,7] which includes also SF and SFS. File CNRF is supplemented by MDF (Mass Differences File) which contains nuclear binding energies ( $E_B$ ), experimental and theoretical as well. A.Arima noticed [8] that future nuclear models will simultaneously describe excitations and  $E_B$ .

According to C.Detraz [9] the existing nuclear models do not contain fundamental information: they have no description of the spilling out of quark interaction through the walls of a quark bag (nucleon), particle properties do not appear in nuclear data. S.Devons [10] suggested that high-quality nuclear data permit to find out fine effects connected with the nucleon structure. Two directions of neutron data study are important:

1) A great number of neutron and charged particle resonance parameters for near-magic nuclei provide the information on properties of few-nucleon configurations which is additional to results obtained by the study of low-lying levels. Numbers of recently measured resonances included in NRF-3 are given in Table 1. Parameters from the SAMMY-fit of cross sections contained in EXFOR also will be included in NRF-3. Table 2 gives numbers of excited states in files CRF (low-lying levels in CNRF), PRF and NRF-2.

2) Neutron resonance data permit to study such fundamental effect in energies of nuclear systems as the correlation between neutron binding energies ( $S_n$ ) and nuclear excitations ( $E^*$ ). The inclusion of  $S_n$  in  $E^*$ -spectrum is the directly measured effect in neutron physics. It reflects the common hadronic origin of both quantities ( $S_B$ ,  $E^*$ ).

**Table 1.** Number of recently measured resonances (target  $AZ$ ).

Isotope $N$	Isotope $N$	Isotope $N$	Isotope $N$	Isotope $N$
$^{35}\text{Cl}$ <span style="border: 1px solid black; padding: 2px;">250</span>	$^{127}\text{I}$ <span style="border: 1px solid black; padding: 2px;">377</span>	$^{192}\text{Pt}$ 154	$^{195}\text{Pt}$ 273	$^{198}\text{Pt}$ 11
$^{37}\text{Cl}$ <span style="border: 1px solid black; padding: 2px;">134</span>	$^{129}\text{I}$ <span style="border: 1px solid black; padding: 2px;">400</span>	$^{194}\text{Pt}$ 246	$^{196}\text{Pt}$ 108	$^{204}\text{Pb}$ many [11]

**Table 2.** Numbers of bound states in compound nuclei  ${}^AZ$  contained in compilations CRF (LB I/19B); the ratio shows the number of states in the books and in Supplement. Numbers of states in compilations of parameters of resonances in reactions with charged particles (LB I/19A) and neutrons (LB I/16C) are given for comparison. Asterisk marks the presence of additional data (EXFOR), their preliminary study was described in [21].

${}^AZ$	19B1	19A 16C	${}^AZ$	19B1	19A 16C	${}^AZ$	19B1	19A 16C
${}^{14}\text{N}$	61/121	154	${}^{38}\text{Cl}$	24/39	37	${}^{55}\text{Mn}$	125/213	374
${}^{15}\text{N}$	21/115	133 61	${}^{36}\text{Ar}$	10/186	179	${}^{56}\text{Mn}$	122/262	175
${}^{16}\text{N}$	14/65	7 47	${}^{38}\text{Ar}$	79/219	578 4	${}^{55}\text{Fe}$	83/183	425*
${}^{15}\text{O}$	8/84	95	${}^{41}\text{Ar}$	57/126	207*	${}^{56}\text{Fe}$	114/271	92
${}^{16}\text{O}$	38/133	215	${}^{39}\text{K}$	34/93	99	${}^{57}\text{Fe}$	136/180	316*
${}^{17}\text{O}$	36/119	70 92	${}^{40}\text{K}$	45/100	70	${}^{58}\text{Fe}$	54/184	127
${}^{18}\text{O}$	31/123	33 15	${}^{41}\text{K}$	123/205	256 39	${}^{59}\text{Fe}$	24/77	82
${}^{17}\text{F}$	36/76	91	${}^{42}\text{K}$	56/171	110	${}^{55}\text{Co}$	100/467	321
${}^{18}\text{F}$	25/100	432	${}^{40}\text{Ca}$	109/580	382	${}^{57}\text{Co}$	105/219	587
${}^{19}\text{F}$	51/190	254	${}^{41}\text{Ca}$	204/271	253	${}^{58}\text{Co}$	152/181	135
${}^{20}\text{F}$	49/152	66*	${}^{42}\text{Ca}$	105/544	415 9	${}^{59}\text{Co}$	20/165	194
${}^{20}\text{Ne}$	28/232	282	${}^{43}\text{Ca}$	111/150	95	${}^{60}\text{Co}$	138/286	221*
${}^{21}\text{Ne}$	33/116	74 102	${}^{44}\text{Ca}$	73/91	55	${}^{59}\text{Ni}$	192/325	576*
${}^{22}\text{Ne}$	65/101	65 45	${}^{45}\text{Ca}$	82/103	65	${}^{60}\text{Ni}$	72/201	22 15
${}^{21}\text{Na}$	14/64	52	${}^{49}\text{Ca}$	26/58	39	${}^{61}\text{Ni}$	230/263	465*
${}^{22}\text{Na}$	36/214	60	${}^{41}\text{Sc}$	25/200	182	${}^{62}\text{Ni}$	68/145	67*
${}^{23}\text{Na}$	73/172	264 1	${}^{42}\text{Sc}$	85/118	112	${}^{63}\text{Ni}$	86/100	81
${}^{24}\text{Na}$	78/119	114*	${}^{43}\text{Sc}$	105/142	315	${}^{65}\text{Ni}$	59/113	58
${}^{24}\text{Mg}$	77/245	385	${}^{45}\text{Sc}$	53/210	1110	${}^{59}\text{Cu}$	107/260	359
${}^{25}\text{Mg}$	56/131	67 64	${}^{47}\text{Sc}$	49/144	294 197	${}^{61}\text{Cu}$	50/126	592
${}^{26}\text{Mg}$	48/204	155 35	${}^{49}\text{Sc}$	149/213	107	${}^{63}\text{Cu}$	114/250	369
${}^{26}\text{Al}$	64/201	146	${}^{46}\text{Ti}$	120/248	106	${}^{64}\text{Cu}$	147/172	291
${}^{27}\text{Al}$	46/243	258 7	${}^{47}\text{Ti}$	95/212	114	${}^{65}\text{Cu}$	42/193	88
${}^{28}\text{Al}$	33/166	260*	${}^{48}\text{Ti}$	118/289	118	${}^{66}\text{Cu}$	97/123	197
${}^{28}\text{Si}$	74/294	314	${}^{49}\text{Ti}$	98/108	87	${}^{65}\text{Zn}$	63/171	402
${}^{29}\text{Si}$	25/129	37 81*	${}^{50}\text{Ti}$	117/259	79	${}^{67}\text{Zn}$	80/129	400
${}^{30}\text{Si}$	31/135	69 31	${}^{51}\text{Ti}$	22/33	34	${}^{68}\text{Zn}$	73/128	504
${}^{31}\text{Si}$	42/74	30	${}^{47}\text{V}$	48/144	282	${}^{69}\text{Zn}$	38/69	292
${}^{29}\text{P}$	15/68	77	${}^{48}\text{V}$	56/81	105	${}^{71}\text{Zn}$	38/38	167
${}^{30}\text{P}$	33/149	97	${}^{49}\text{V}$	94/254	1213	${}^{83}\text{Kr}$	25/77	176
${}^{31}\text{P}$	127/171	504	${}^{50}\text{V}$	150/180	98	${}^{85}\text{Kr}$	26/76	207
${}^{32}\text{P}$	147/147	33*	${}^{51}\text{V}$	117/213	322 18	${}^{87}\text{Kr}$	17/169	225*
${}^{32}\text{S}$	146/256	315	${}^{52}\text{V}$	79/131	153*	${}^{91}\text{Zr}$	99/157	141*
${}^{33}\text{S}$	27/151	156 105	${}^{51}\text{Cr}$	152/269	382	${}^{92}\text{Zr}$	84/135	145*
${}^{34}\text{S}$	39/133	104 60	${}^{53}\text{Cr}$	51/166	341	${}^{93}\text{Zr}$	69/69	101*
${}^{35}\text{S}$	36/59	82	${}^{54}\text{Cr}$	35/138	124	${}^{95}\text{Zr}$	59/63	73*
${}^{34}\text{Cl}$	33/120	194	${}^{55}\text{Cr}$	64/106	111	${}^{135}\text{Ba}$	82/99	90*
${}^{35}\text{Cl}$	134/248	224	${}^{51}\text{Mn}$	40/140	406	${}^{206}\text{Tl}$	81/94	139*
${}^{36}\text{Cl}$	92/127	84	${}^{53}\text{Mn}$	153/416	973	${}^{208}\text{Pb}$	264/583	382*
${}^{37}\text{Cl}$	28/84	422 16	${}^{54}\text{Mn}$	79/146	281	${}^{209}\text{Pb}$	167/217	94*

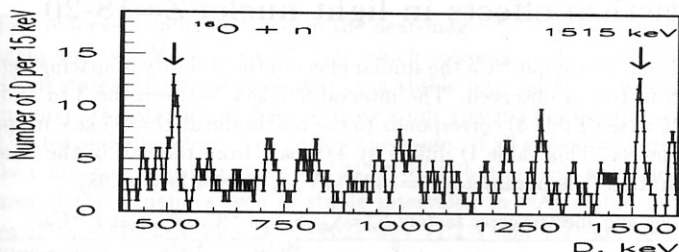


Fig. 1. Nonstatistical effect in spacing distribution of  $^{16}\text{O}$  resonances found by M.Ohkubo.

An example of the presence of stable intervals in neutron resonances was found recently by M.Ohkubo [12]: see Fig.1 where the grouping effect in spacing of states in  $^{17}\text{O}$  (or resonances in  $^{16}\text{O}$ ) occurs at  $D$  about 500 and 1515 keV (see other results in [12]).

The low energy part of the file CNRF is based on CRF-file which contains the existing information on the spectroscopic factors ( $S$ ) of all nuclei. Together with magnetic moments, factors  $S$  are the basic elements needed for the understanding of nuclear structure.  $S$  is defined as the probability to reach a final single-particle (hole) state when a nucleon is added to (or removed from) the target nucleus. The occupation number is the number of nucleons in the certain quantum state in the target nucleus, relative to the  $2j + 1$  limit. The common method of data analysis includes a comparison with calculations by Distorted Waives Born Approximation (DWBA). The measured cross section  $\sigma_{exp}$  and the transfer reaction spectroscopic factor  $S$  (e.g.  $S_{dp}$  for deuteron stripping) are connected with the theoretically estimated cross section  $\sigma_{DWBA}$  by the relation:

$$\sigma_{exp} = (2J + 1)(2I + 1)^{-1}(2j + 1)^{-1} \times S_N \times N \times \sigma_{DWBA}$$

with  $N$  – theoretical normalization parameter,  $J, I, j$  – moments of states and nucleon.

In [13] from the large values of the observed spectroscopic factors and the constancy of excitations (boxed values in Table 2) it was concluded that single-particle approximation is valid in such near-magic nuclei as  $^{40}\text{K}$ ,  $^{40}\text{Ca}(T=1)$ ,  $^{40}\text{Sc}$ . This observation means that a study of stable excitations of levels with the large spectroscopic factors can provide the important information needed for development of the nuclear shell model. We apply this method of data-analysis to the observed stability (within several keV) of excitation  $\approx 894$  keV in nuclei around  $A=40$  (Table 2). It was found earlier [14] that in sum distribution of excitations of all nuclei with  $A \leq 70$  there is the grouping effect at  $E^* = 888$  keV (Fig.2). In the  $E^*$ -distribution for all near-magic nuclei with  $Z=19, 21, 27, 29$  (proton shells  $Z=20, 28$ ) the grouping effect takes place at four-fold value  $E^* = 894 \times 4 = 3577$  keV (see Fig.2) [6,15]. The role of neutron resonance data in the systematic study of such kind of nonstatistical (tuning) effects in spacing of levels in the near-magic nuclei is discussed here.

Table 3. Energies and  $S_{dp}$  of members of the lowest multiplet for  $A=40$ ,  $T=1$  [13,14].

$J^\pi$	$^{40}\text{K}$		$^{40}\text{Ca}(T=1)^{**}$		$^{40}\text{Sc}$		Comments Energies in keV
	$E_{exp}^*$	$S_{dp}$	$E_{exp}^*$	$E_{theor}^*$	$E_{exp}^*$	$E_{theor}^*$	
$4^-$	0	0.9	0	1	0	39	Energies in $^{40}\text{Ca}$ ( $T=1$ ) are after subtracting 7658 keV.
$3^-$	30	0.9	36	24	34	34	
$2^-$	800	0.9	767	773	772	772	
$5^-$	891	0.8	893	864	894	859	

## 2 Nonstatistical effects in light nuclei $Z=18-20$

In other near-magic nuclei around  $^{40}\text{Ca}$  the similar effect of the stability of spacing between states with large S-factors is observed. The interval 897 keV between the 3-rd and 4-th excited states of  $^{43}\text{Ca}$  (see Table 3) corresponds to the maximum at  $D=895$  keV in spacing distribution of all levels. This value  $D$  differs by  $1/8$  part from the half of the observed single-particle excitation (the parameter  $\varepsilon_0=1022$  keV,  $\varepsilon_0/\varepsilon_0-894$  keV=7.98).

**Table 4.** Excitations and spectroscopic factors  $S_n^+=S_{dp}, S_{\alpha\tau}$  of  $^{43}\text{Ca}$ ,  $^{38}\text{Ca}$  and  $^{42}\text{Ca}$ .

$^{43}\text{Ca}$						$^{38}\text{Ca}$	$^{42}\text{Ca}$	Comments	
$2J^\pi$	$E_{exp}^*$	diff.	$S_{dp}$	$S_{\alpha,\tau}$	$D$	$J^\pi$	$E_{exp}^*$	$E_{exp}^*$	Energies in keV
$7^-$	0		4.5	5.4	342	$0^+$	0	0	$341=(1/3)\varepsilon_0$
$5^-$	373		3.9	0.15		$2^+$	2206	1524	$2044=2\varepsilon_0$
$3^-$	2046	897	2.9	4.3	895	$0^+$	3057(18)	1837	$3066=3\varepsilon_0$
$3^-$	2943		0.19	0.74	2942	$2^+$	3685	2424	$894=(7/8)\varepsilon_0$

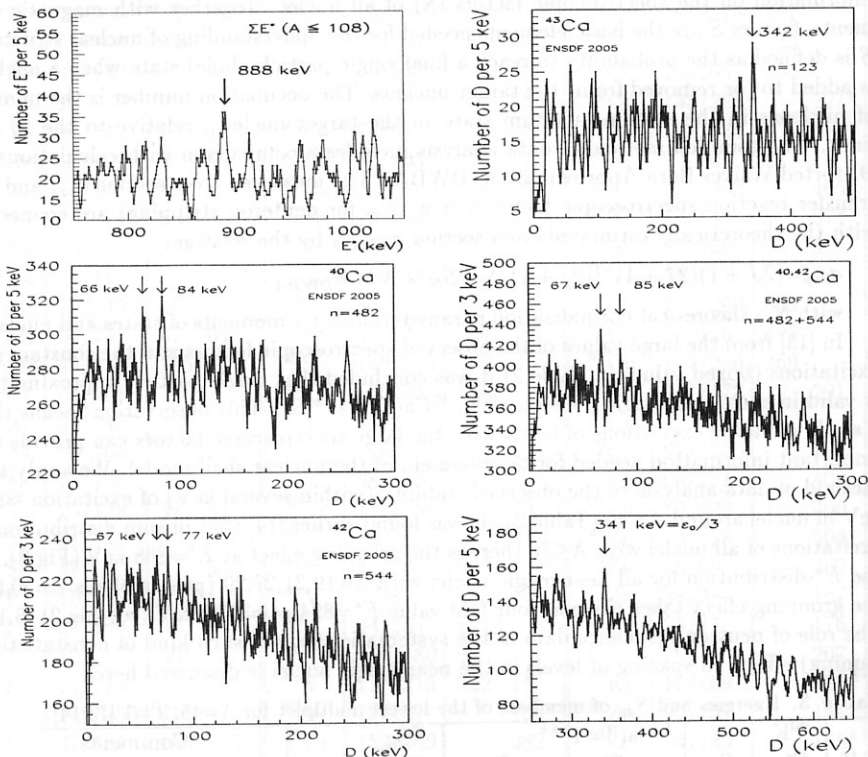


**Fig. 2** *Top left:* Distribution of excitation energies of nuclei with  $A=4-108$  (ENSDF 1993) [14]. *Top right:* Spacing distribution in energy levels of  $^{43}\text{Ca}$  (ENSDF 2005). *Center:*  $D$ -distribution in  $^{40}\text{Ca}$  and sum spacing distribution in  $^{40}\text{Ca}$  and  $^{42}\text{Ca}$ . *Bottom left:* Spacing distribution in energy levels of  $^{42}\text{Ca}$  (ENSDF 2005). *Bottom right:* Sum spacing distribution in neutron resonances of target  $^{40}\text{Ca}$  and  $^{42}\text{Ca}$ .

Two observed stable intervals in the near-magic  $^{38}\text{Ar}$  (Fig.3 top) were studied by the Adjacent Interval Method (AIM) [14] which consists in the following. First we collect in PC all states which are separated by a stable interval  $D=x$  (within  $\Delta E$ ) forming the maximum in  $D$ -distribution. Secondly, we study spacing distribution ( $D^{AIM}$ ) between the fixed states and all states in the energy spectrum. If all states (or part of them) separated by  $D=x$  are distinguished, then the  $D^{AIM}$ -distribution will show additional systematic features of the dynamics seen in stable intervals. In  $^{38}\text{Ar}$  stable  $D^{AIM}$  rational to the values  $D=x=1476$  keV and  $D=x=1021$  keV (1:2:3 and 1:2) are seen in Fig.3 (center). Stable intervals in  $^{20}\text{F}$  and  $E^*$  in nuclei with  $Z\leq 70$  seen as maxima in Fig.3 (bottom) correspond to the discussed system of intervals  $n=1:2:3:6$  with a period 492 keV.

**Table 5.** Excitations in light nuclei from  $^{33}\text{S}$  up to  $^{39}\text{Ca}$  [14].

$^{33}\text{S}$	$^{38}\text{Cl}$	$^{39}\text{K}$	$^{37}\text{Ar}$	$^{38}\text{Ar}$	$^{39}\text{Ca}$	$^{41}\text{K}$	Comments
$2J^\pi$	$E_{exp}^*$	$E_{exp}^*$	$E_{exp}^*$	$E_{exp}^*$	$E_{exp}^*$	$D^{AIM}$	$E^*$ in keV
$3^+$	0	0	0	0	0		$984=13\times 8\delta'$
$5^+$	1967	2523	1410	2167	2469		$1968=2\times 984$
$3^+$	3935	3938	3939	3937	3936	3940	$3939=13\times 303$

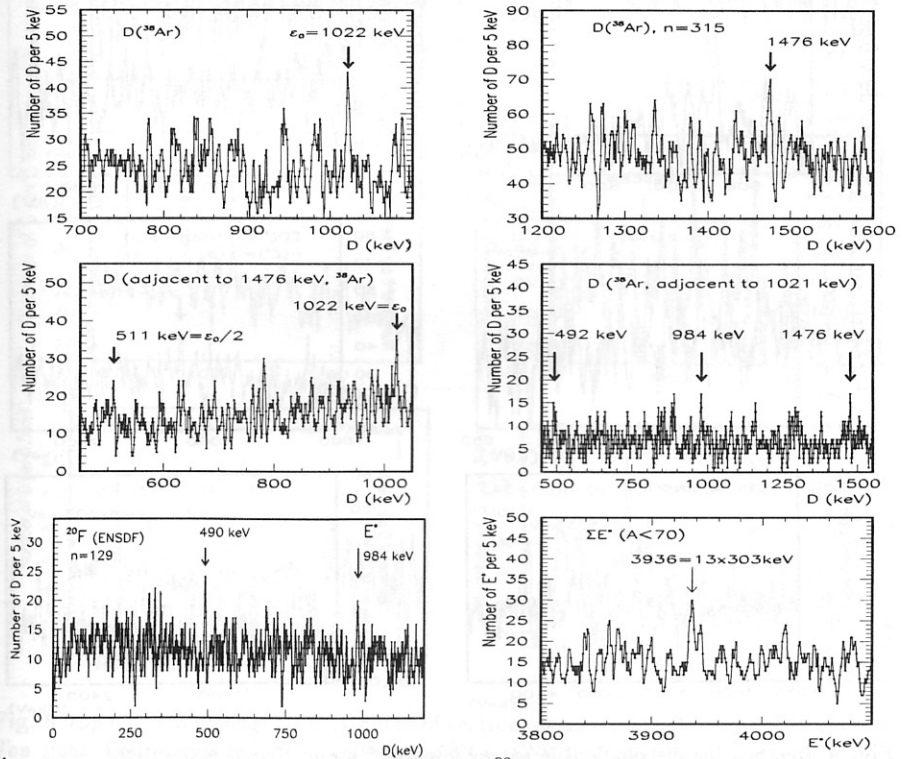


**Fig. 3** Top: Two maxima in spacing distribution of  $^{38}\text{Ar}$  energy levels (ENSDF) [14].

Center:  $D^{AIM}$ -distribution in  $^{38}\text{Ar}$  for stable intervals  $x=1476$  and 1021 keV [14].

Bottom left: Spacing distribution in energy levels of  $^{20}\text{F}$  (ENSDF) [6].

Bottom right: Total distribution of excitations in nuclei with  $Z\leq 70$  [14].

We observe other manifestation of the discussed systematics with the parameter of tuning effect  $\varepsilon_o (=2m_e=1022 \text{ keV})$  in excitations of the near-magic nuclei around  $^{40}\text{Ca}$ :

Maxima at the same  $D=637 \text{ keV}$  in two nuclei  $^{18}\text{F}$  and  $^{22}\text{Na}$  (differing by  $\alpha$ ) are shown in Fig.4 (top). These values are close to a half of the first excitation of the neighbour  $^{22}\text{Ne}$   $E^*=1274.5 \text{ keV}$  ( $5/4\varepsilon_o=5110/4=1277 \text{ keV}$  (Table 4).

In  $^{42}\text{Ca}$  a stable spacing  $D=\varepsilon_o/2=511 \text{ keV}$  (Fig.4 center) was discussed in [16].

In  $^{41}\text{K}$  (also  $N=22, Z=20-1$ ) stable spacing  $D=2\varepsilon_o=2044 \text{ keV}$  (close to the single-particle excitation in  $^{43}\text{Ca}$ , Table 3) and  $D=3940 \text{ keV}$  (close to  $E^*$ -grouping) are clearly seen in Fig.4 together with the result of the AIM-analysis for  $x=D=2044 \text{ keV}$  which showed stability of  $D^{AIM}=2424 \text{ keV}$  and  $D^{AIM}=6060 \text{ keV}$  (which forms triplets with  $D^{AIM}=1515 \text{ keV}$  [14]). The integer relations with the period  $303 \text{ keV}$  between intervals  $D=1515:2424:6060 \text{ keV}$ , common excitations  $E^*=3938 \text{ keV}$  and  $1212 \text{ keV}$  and  $0^+$  excitations in  $^{16}\text{C}$  ( $3026 \text{ keV}$ ),  $^{16,18}\text{O}$  ( $6050 \text{ keV}$ ,  $3634 \text{ keV}$ ) and  $^{46}\text{Ca}$  ( $2423 \text{ keV}$ ) were earlier discussed in [6,14]. The interconnection between these intervals and other intervals of the fine structure are discussed in [17].

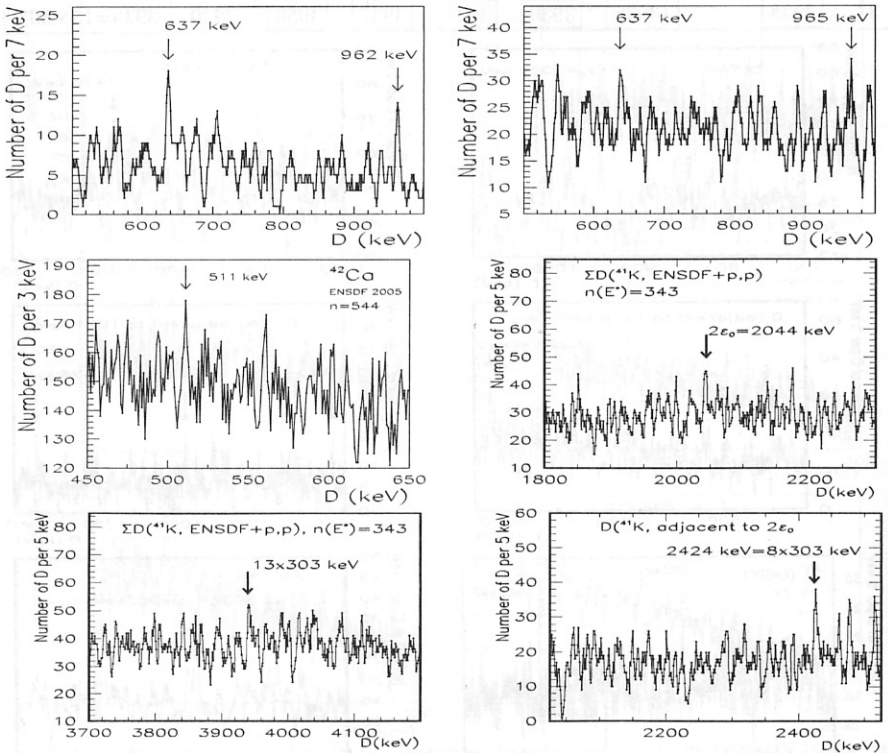


**Fig. 4** Top: Spacing distributions in energy levels of  $^{18}\text{F}$  and  $^{22}\text{Na}$  (ENSDF) [7].

Center left: Spacing distribution in energy levels of  $^{42}\text{Ca}$  (ENSDF 2005).

Center right and bottom left: Spacing distribution in energy levels of  $^{41}\text{K}$  (ENSDF) [14].

Bottom right: Distribution of adjacent intervals ( $D^{AIM}$ ) for  $x=D=2044 \text{ keV}$  in  $^{41}\text{K}$  [14].

### 3 Nonstatistical effects in light nuclei $Z=24-29$

Fine structures in D-distributions found in the recent data for bound states of  $^{40,42}\text{Ca}$  (Fig.2  $D=n\delta'$ ,  $n=7,8,9$ ;  $\delta'=9.5$  keV) is similar to that found earlier in positions of resonances of light nuclei (at 18.8 keV), in D-distribution in states of  $^{55}\text{Co}$  ( $D=84$  keV  $\approx 9\delta'$ ) and resonances of  $^{51}\text{Cr}$  ( $D=n\delta'$  with  $n=4,9,13,17,18$ ; see Fig 5). D-distribution of  $^{56}\text{Fe}$  resonances demonstrates the stability of intervals 33 and 66 keV= $7\delta'$  while in the same data the AIM-method (see 3 parts of Fig.6) permits to notice  $D^{AIM}=85-170-255$  keV from another series  $n \times 9\delta'$ . In D-distribution of  $^{59}\text{Co}$  resonances (Fig.6 bottom) we see splitting of  $D=16.5$  keV= $7\delta'/4$  by intervals 4.3 keV  $\approx (1/4)16.5$  keV.

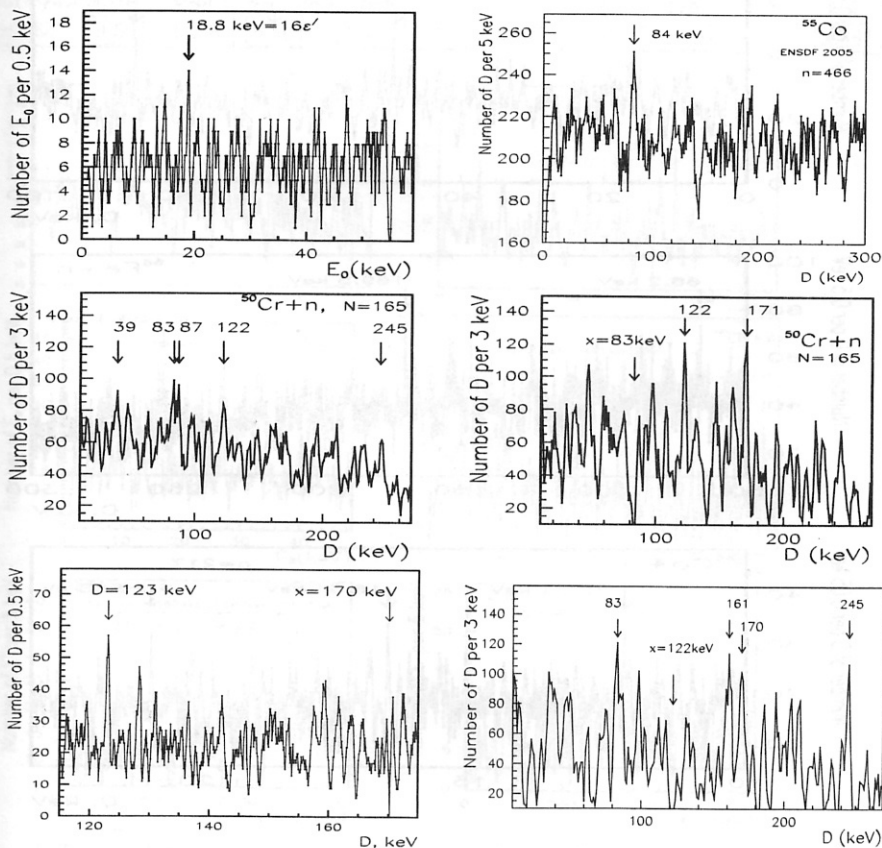


**Fig. 5** *Top left:* Grouping effect in positions of neutron resonances of light nuclei at 19 keV= $2\delta'$ . *Top right:* Distribution of intervals in levels of  $^{55}\text{Co}$  (ENSDF 2005). *Center left:* Spacing distribution between all resonances with negative parity in compound nucleus  $^{51}\text{Cr}$  with maxima at 39 keV= $4\delta'$ , 83 and 87 keV ( $\approx 9\delta'$ ) and 123 keV ( $13\delta'$ ). *Center right and bottom:* Distribution of intervals in  $^{51}\text{Cr}$  adjacent to  $x=D=83$  keV,  $x=170$  keV and  $x=122$  keV. All intervals including 161 keV= $17\delta'$  and 170 keV= $18\delta'$  are marked.

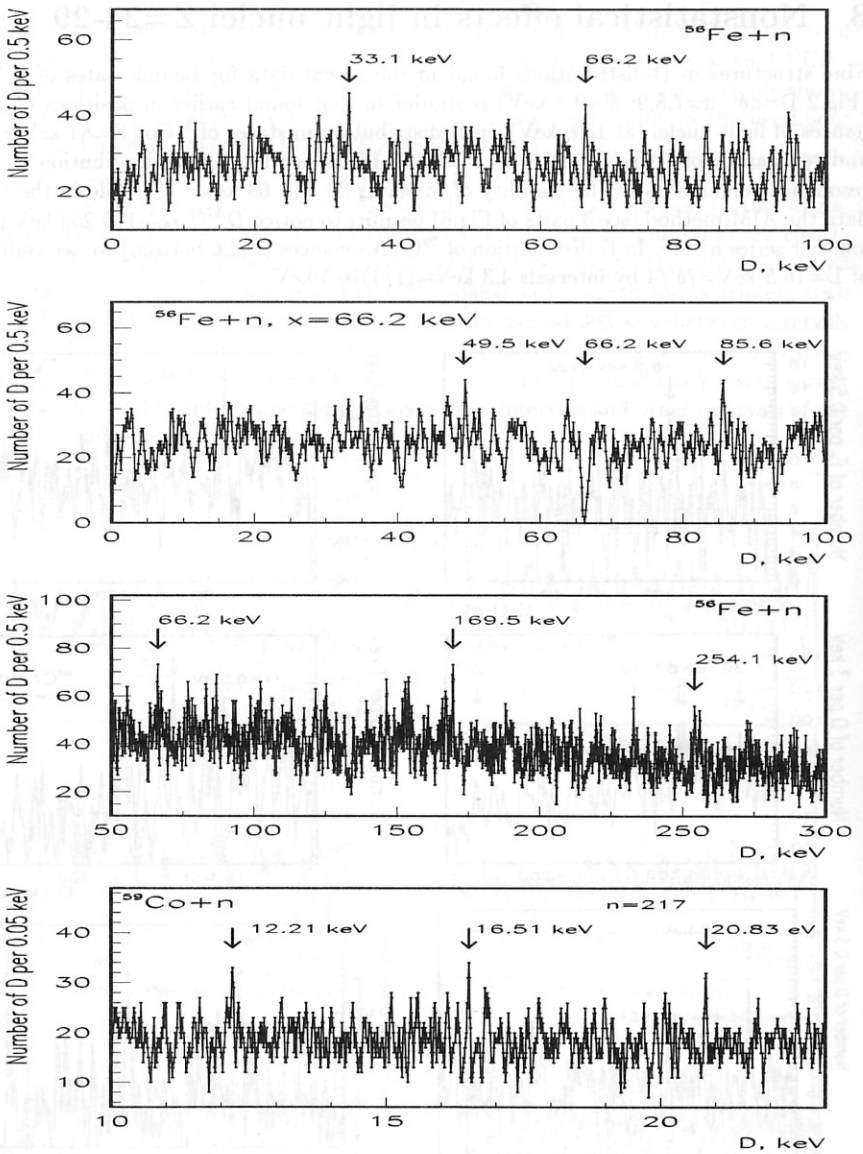


**Fig. 6.** Top: Sum spacing distribution between s- and p-resonances of target  $^{56}\text{Fe}$ .  
 The 2-nd part: D-distribution between all resonances of  $^{56}\text{Fe}$  adjacent to  $D=x=66.2$  keV.  
 Center: Spacing distribution between all resonances of target  $^{56}\text{Fe}$  adjacent to  $132=133$  keV.  
 Bottom: Spacing distribution between all resonances of target  $^{59}\text{Co}$ .



## 4 Nonstatistical effects in nuclei with $Z=38-58$

Noticed by M.Ohkubo [18, 19] relation  $9/4$  in positions of strong neutron resonances in  $^{141}\text{Ce}$  and the grouping of resonances in  $^{82}\text{Br}$  are compared in Table 6 with  $\delta'=9.5$  keV and the splitting of levels of  $^{143}\text{Ce}$  due to the residual interaction of valence neutrons.

**Table 6** [20]. Positions of strong resonances in nuclei with  $N=83$ ,  $Z=57-59$  and  $Z=35,37$  in the comparison two with excitations in  $^{143}\text{Ce}$  ( $N=82+3$ ).

Nucl.	$^{141}\text{Ce}$	$^{142}\text{Pr}$	$^{140}\text{La}$	$^{143}\text{Ce}$	$3/2^-$	$5/2^-$	$^{141}\text{Ce}$	$^{80}\text{Br}$	$^{82}\text{Br}$	$^{86}\text{Rb}$
$J_i^\pi$	$1/2^+$	$1/2^+$	$(5/2^-)$	$3^+$	$7/2^-$	$5/2^-$		$l_n=0$	$l_n=0$	$l_n=0$
$\Gamma_n^o, \text{mV}$	660	3060	160	54				72.0	120	159
$E^*, E'_n$	9.50	21.41	9.53	1.17	18.9	42.28		1.19	1.19	2.37
$m(\delta')$	1	$9/4$	1	$1/8$	2	$9/2$	$9/4$	$1/8$	$1/8$	$1/4$
$m \times 8\delta'$	9.50	21.38	9.50	1.19	19.0	42.77	21.4	1.19		2.38

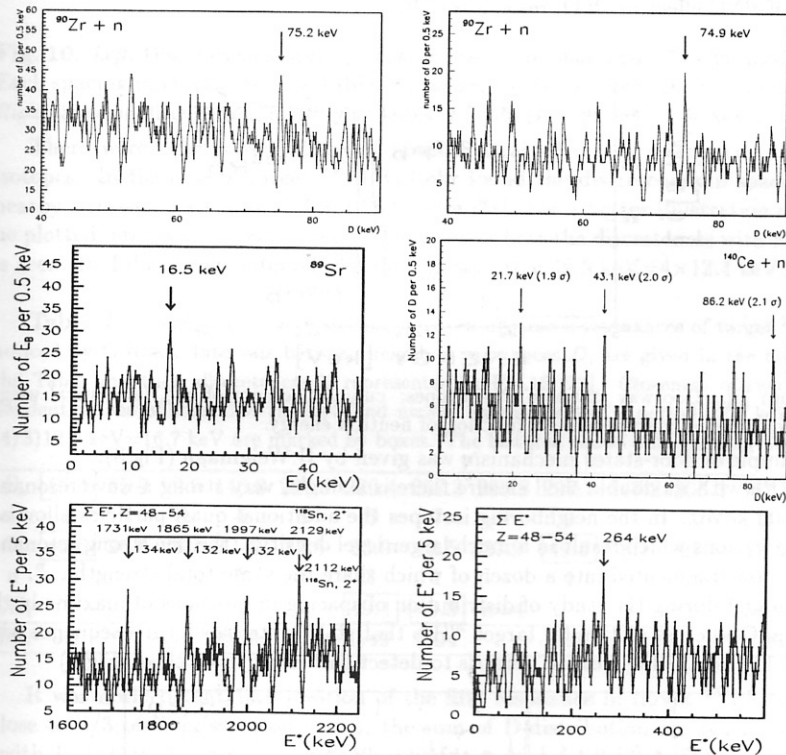


**Fig. 7** Top: D-distribution in neutron resonances of target  $^{90}\text{Zr}$  ( $D=75$  keV  $\approx 8\delta'$ ) and the same for spacing between positions of maxima in total neutron cross section of  $^{90}\text{Zr}$  [21]. Center: D-distributions in neutron resonances of compound nucleus  $^{88}\text{Sr}$  at  $D=16.5$  keV  $=66$  keV/4  $=7\delta'/4$  and compound nucleus  $^{141}\text{Ce}$  at  $D=21.5$  keV  $=85$  keV/4  $=9\delta'/4$ . Bottom:  $E^*$ -distribution for all nuclei with  $Z=48-54$  in two energy regions, the marked periodicity has an interval  $133$  keV  $=27\delta'$ ; the maximum at  $264$  keV is close to  $2 \times 133$  keV [15].

The coincidence of positions (at  $\delta'=9.5$  keV) of the strong resonances in both target nuclei with magic number  $N=82$  ( $^{141}\text{Ce}$  and  $^{142}$  in Table 6) means that the parameter  $\delta'$  corresponds to the common tuning effects in  $E^*$  and  $E_B$ . Its value and the parameter  $(1/8)\delta'=\varepsilon'=1.19$  keV from  $E'_n$  in  $^{80,82}\text{Br}$ ,  $^{86}\text{Rb}$  and  $^{140}\text{La}$  (Table 6) are discussed in [17].

In Fig.7 stable intervals in resonances of the target  $^{140}\text{Ce}$ ,  $^{90}\text{Zr}$  and  $^{88}\text{Sr}$  as well as the grouping effect in excitations ( $E^*$ ) of all nuclei around tin ( $Z=48=54$ ) are compared with the integer numbers of the parameter of fine structure  $n\delta'$  ( $n=8, 7/4, 9/4$  and  $27$ ).

## 5 Nonstatistical effects in lead region

The idea of "doorway states" for a description of small splittings in values of nuclear excitations was put forward by H.Feshbach and supported by E.Wigner. This model connects small splittings at high-energy excitations with the real intervals in low-lying levels of the same or neighbour nuclei. For example, it was used for explaining of nonstatistical character of PNC-effect in  $^{232}\text{Th}$  resonances [3].

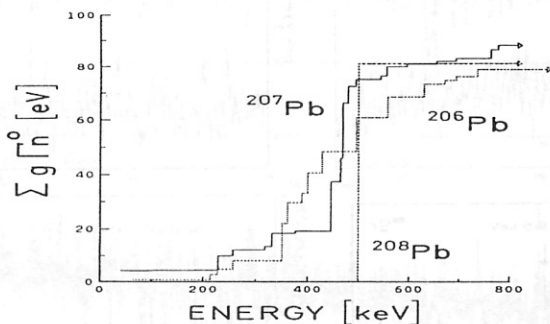


Fig. 8 from [3]. Doorway states in Pb-isotopes: cumulative sum of  $g\Gamma_n^0$  (statistical weight factor  $\times$  reduced neutron width) as a function of neutron energy.

An example of door-states mechanism was given by H.Weigmann (Fig.8):

" In  $^{208}\text{Pb}$  with its double shell closure there is a single, very strong s-wave resonance at about 500 keV ... In the neighboring isotopes the additional quasi-particles allow additional excitations which result in a much larger level density... the one strong resonance of  $^{208}\text{Pb}$  is now fragmented into a dozen of which share the same total strength ..."

It was found during the study of distribution of spacing in positions of maxima in the measured in Geel cross section for target  $^{207}\text{Pb}$  that stable intervals form a sequence with the period 128 keV. AIM-method permits to detect this effect more clear (Fig.9)

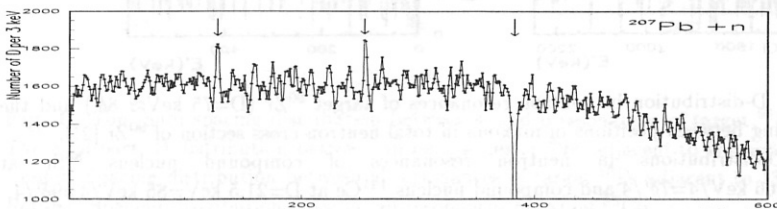


Fig. 9 Distribution of intervals in neutron resonances of target  $^{207}\text{Pb}$  adjacent to  $D=x=383$  keV. Arrows indicate  $D^{AI}=128$  and  $255$  keV. All values can be expressed as  $n \times (1/8)\varepsilon_0$  ( $n=1,2,3$ ).

LEVEL SPACINGS IN UNITS OF 12.4 keV

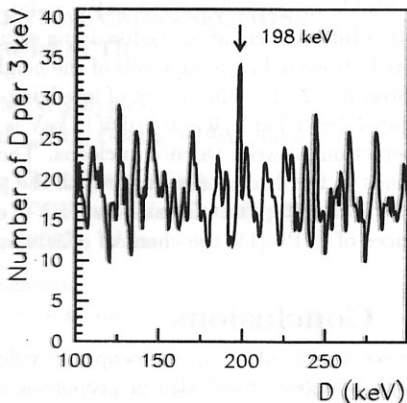
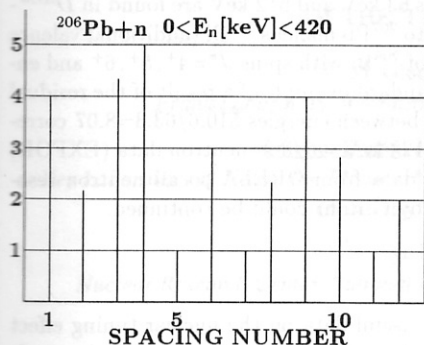


Fig. 10. Left: Discreteness in spacing between neutron resonances of  $^{206}\text{Pb}$  noticed by G.Rohr. Each spacing in this figure (see Table 7) is shown by the vertical line in units of 12.4 keV. Right: Spacing distribution in low-lying levels of  $^{205}\text{Pb}$  ( $D=198\text{ keV}=3\cdot 66\text{ keV}$ ).

There were other observations of nonstatistical effects in resonances data for lead isotopes. In the case of target  $^{206}\text{Pb}$  G.Rohr found the discreteness in spacing between nearby s-resonances shown in Fig.10 left from [21]. For a better illustration of this effect he plotted intervals as vertical lines in the figure where the discreteness with a period 12.4 is seen. In Table 7 four intervals with the mean value  $49.5\text{ keV}=4\times 12.4\text{ keV}$  are boxed.

Table 7. Integer relations in spacing between neutron s-resonances of target  $^{206}\text{Pb}$  [22,13] noticed by G.Rohr. Intervals between neighbor resonances  $D_i$  are given in the middle part of the Table and their discreteness is represented in Fig.10 [22]. Closeness of two  $D_i$  to independent values of sum  $\Sigma D_i$  ( $n=1+3$  and  $n=3+1$  in numbers of a period 12.5 keV) and  $E_o \approx (4/3)12.5\text{ keV}=16.7\text{ keV}$  are marked by boxes. The last line shows difference  $D_i-n(49.5\text{ keV}/4)$ .

$E_o$	16.4	65.9	92.6	146.3	207.9	220.4	257.3	269.8	297.7	347.2	355.3	382.8	395.1
i	1	2	3	4	5	6	7	8	9		10	11	12
$D_i$	49.6	26.6	53.7	61.6	12.5	36.9	12.5	27.9	49.5	8.1	27.5	12.2	24.7
n	4			5	1	3	1		4			1	2
$\Sigma D_i$						49.4	49.3	n=4				36.9	n=3
diff.	0.1			0.65	0.09	0.49	0.04		0.0			0.23	

It was noticed that 1) a position of the first resonance in target  $^{206}\text{Pb}$  (16.4 keV) is close to  $4/3$  of Rohr's period and 2) the sum of D-distribution for s- and p-resonances (with  $J=3/2$ ) in the same target  $^{206}\text{Pb}$  contains maxima at  $n=3$  4 of the period 12.4 keV. Stable interval  $D=198\text{ keV}=3\times 66\text{ keV}=3\times 7\delta'$  was found in spacing of low-lying levels of the neighbor  $^{205}\text{Pb}$  (Fig.10 right, averaging  $\Delta E=3\text{ keV}$ , rms deviation  $\approx 3\sigma$ ).

We could mention the fact that stable intervals  $D=49\text{ keV}$  and  $73\text{ keV}$  close to four- and sixfold values of Rohr's period are seen in the spacing distribution of all low-lying levels of the same compound nucleus  $^{207}\text{Pb}$ . These and additional stable  $D=247\text{ keV}=5\times 49.5\text{ keV}$  and  $D=497\text{ keV}=10\times 49.5\text{ keV}$  are forming triplets seen as maxima in  $D^{AIM}$ -distributions.

Stable intervals  $D=49-73$  keV similar to that found in Rohr's nonstatistical effect as well as intervals equal to the low-lying excitations 63 keV and 512 keV are found in  $D^{AIM}$ -distributions in low-lying levels of the neighbour to  $^{207}\text{Pb}$  nucleus  $^{208}\text{Bi}$  (additional valence proton  $Z=82+1$ ). The triplet of low-lying levels of  $^{208}\text{Bi}$  with spins  $J^\pi=4^+, 5^+, 6^+$  and energies  $E^*=63.3$  keV, 0 and 510.6(1) keV is the standard example of a result of the residual interaction between valence nucleons. The ratio between energies  $510.6/63.3=8.07$  corresponds to the discussed relation with the period  $128 \text{ keV}=\varepsilon_o/8$  in neutron data (EXFOR) for  $^{208}\text{Pb}$ . After the inclusion in NRF-3 of new data from ORELA on all neutron resonances of  $^{204}\text{Pb}$  [11] the check of effects noticed by G.Rohr could be continued.

## 6 Conclusions

We see that neutron spectroscopy provides very useful data on the nuclear tuning effect which manifests itself also in properties of bound states. The study of stable intervals in low-lying levels due to the residual interaction of valence nucleons is, according to the door-way states model, the natural method for the study of the so-called nonstatistical effects. We see the difference in methods of data-analysis: the statistical approach uses normalized values but to consider a real dynamics one should use the absolute scale.

## References

1. S.F.Mughabghab *et al.*, Neutr. Cross Sections, v.1 (1981-1984); www.nndc.bnl.gov
2. S.I.Sukhoruchkin, Z.N.Soroko, V.V.Deriglazov, "Tables of neutron resonance parameters", L-B New Series, vol. 1/16B, Springer, 1998. Ed. H.Schopper.
3. A.Brusegan, F.Corvi, P.Rullhusen, S.I.Sukhoruchkin, Z.N.Soroko, H.Weigmann, "Tables of neutron resonance parameters", L-B New Series, vol. 1/16C, Springer, 2004. Ed. H.Schopper.
4. W.Martienssen, Landolt-Börnstein Complete Catalog, p.3. Springer, 2000.
5. Z.N.Soroko, S.I.Sukhoruchkin, Proc.ISINN-6, 1997, JINR E3-98-202, p.141.
6. Z.N.Soroko *et al.*: Proc.ISINN-10, 2002, JINR E3-2003-10, pp.289, 299,308.
7. S.I.Sukhoruchkin: Proc.ISINN-8, 2000, JINR E3-2000-192, p.428.
8. A.Arima, Nucl. Phys. A **680**, 305c (1990).
9. C.Detraz, Nucl. Phys. A **583** 3, (1995).
10. S.Devons, Proc. Rutherford Jubilee Int. Conf., Manchester, Ed.J.Birks, Heywood, p.611.
11. Carlton, R.F., Harvey, J.A., Hill, N.W., PRC **67** (2003) 024601.
12. Ohkubo, M : Proc. Symp. Nucl. Data, 2002, Tokai, JAERI-Conf. 2003-006, p. 259.
13. Fortune, H.T., Sherr, R.: Phys. Rev. C **65** (2002) 067301.
14. Soroko, Z.N., Sukhoruchkin, S.I.: Proc. 7th Int. Seminar on Interact. Neutr. Nucl. ISINN-7, Dubna, 1999. JINR E3-99-212 p. 313.
15. S.I.Sukhoruchkin, Proc. 11th Int. Symp. Capture Gamma-Rays, Czech Rep., 2002. World Sci., 2003, pp.825, 829.
16. S.Sukhoruchkin, D.Sukhoruchkin, Nucl. Phys. A **722** (2003) 553c.
17. S.Sukhoruchkin, this Proceedings.
18. Ohkubo, M., Mizumoto, M., Nakajima, Y.: Rep. JAERI-M-93-012, 1993.
19. Ohkubo., M. et al.: J. Nucl. Sci. Techn. (Tokyo) 18, 745 (1981).
20. Z.Soroko, S.Sukhoruchkin, D.Sukhoruchkin, JNST (Tokyo) Suppl.2 (2002), p.p.64, 504.
21. Soroko, Z.N., Sukhoruchkin, S.I.: Proc.ISINN-9, Dubna. JINR E3-2001-192, pp. 334,342.
22. Rohr, G.: Proc. 8th Symp. Capt. Gamm-Rays, Fribourg, 1993. World Sci., p.626 (1994).